

LARGE EDDY SIMULATIONS OF SPRINKLER, VENT AND DRAFT CURTAIN PERFORMANCE

by

**Kevin McGrattan and David Stroup
Building and Fire Research Laboratory
National Institute of Standards and Technology
Gaithersburg, MD 20899, USA**

**Reprinted from the Fire Suppression and Detection Research Application Symposium.
Research and Practice: Bridging the Gap, February 12-14, 1997, Orlando, FL, 59-68 pp.
Proceedings. National Fire Protection Research Foundation, 1997.**

**NOTE: This paper is a contribution of the National Institute of Standards and
Technology is not subjected to copyright.**

Large Eddy Simulations of Sprinkler, Vent and Draft Curtain Performance

Kevin McGrattan and David Stroup
Building and Fire Research Laboratory
National Institute of Standards and Technology
Gaithersburg, Maryland 20899

The National Fire Protection Research Foundation (NFPRF) is overseeing a project to evaluate the interaction of sprinklers with draft curtains and smoke/heat vents. The goal of the project is to develop an engineering method capable of quantifying the conditions under which vents and draft curtains are beneficial, and under which they are detrimental, to the performance of a sprinkler system in large enclosures. To reach the goal, full scale commodity fires are being planned for a space that will mimic as much as possible large storage and manufacturing facilities. Towards that end, 22 heptane spray burner tests were conducted in January, 1997, at the Underwriters Laboratories large-scale fire test facility to study the interaction between sprinklers, vents and draft curtains in a well-controlled environment. One of the objectives of these tests was to evaluate the predictive capability of a field model presently under development at the National Institute of Standards and Technology (NIST). The model, which is referred to as the NIST Large Eddy Simulation (LES) fire model [1, 2, 3], is a computational fluid dynamics code that solves the equations governing the flow of smoke and hot gases from a fire. Phenomena like sprinkler sprays, flame spread and radiative transport have been incorporated in the model.

The purpose of this paper is to discuss the numerical model and some sample calculations of the UL heptane burner tests. The degree to which the model is able to replicate the experimental results will determine to what extent it can be used as a tool to expand the experimental test matrix beyond its limited number of tests, and also to plan the next series of tests.

Mathematical Model

Consider a thermally expandable ideal gas driven by a prescribed heat source. The equations of motion governing the fluid flow are written in a form suitable for low Mach number applications [4]. Sometimes, this form of the equations is referred to as "weakly compressible". The most important feature of these equations is that in the energy conservation equation the spatially and temporally varying pressure is replaced by an average pressure p_0 which depends only on time. This is done to filter out acoustic waves. The efficiency of the numerical solution of the equations is dramatically increased by this approximation.

In the equations to follow, all symbols have their usual fluid dynamical meaning: ρ is the density, \mathbf{u} the velocity vector, $\boldsymbol{\omega}$ the vorticity, p the pressure, \mathbf{g} the gravity vector, c_p the constant-pressure specific heat, T the temperature, k the thermal conductivity, t the time, \dot{q} the prescribed volumetric heat release, \mathcal{R} the gas constant equal to the difference of the specific heats $\mathcal{R} = c_p - c_v$, \mathcal{F} an external force term, and $\boldsymbol{\sigma}$ the standard stress tensor for compressible fluids.

$$\frac{\partial \rho}{\partial t} + \nabla \cdot \rho \mathbf{u} = 0 \quad (1)$$

$$\rho \left(\frac{\partial \mathbf{u}}{\partial t} + \frac{1}{2} \nabla |\mathbf{u}|^2 - \mathbf{u} \times \boldsymbol{\omega} \right) + \nabla p - \rho \mathbf{g} = \mathcal{F} + \nabla \cdot \boldsymbol{\sigma} \quad (2)$$

$$\rho c_p \left(\frac{\partial T}{\partial t} + \mathbf{u} \cdot \nabla T \right) - \frac{dp_0}{dt} = \dot{q} + \nabla \cdot k \nabla T \quad (3)$$

$$p_0(t) = \rho \mathcal{R} T \quad (4)$$

The numerical solution of these equations is described in Ref. [5]. Of importance to the discussion at hand are the sources and sinks of energy. The source is obviously the fire, and the sinks consist of the sprinkler sprays, walls, and vents.

The fire is represented by introducing a large number of Lagrangian elements which release heat as they are convected about by the thermally induced motion. Since the fluid motion determines where the heat is actually released, and the heat release determines the motion, the large scale features of the coupling between the fire and the smoke transport are retained. It should be noted, however, that the heat release rate is *not* predicted, but is an input parameter in the computer programs implementing this model. The smoke is simulated by tracking the convected elements after the fuel burnout is completed. A specified percentage of the fuel consumed is assumed to be converted to smoke particulate. Thus, a knowledge of the spatial distribution of the Lagrangian elements is equivalent to a specification of the smoke particulate density at any instant of time. This "thermal element" model, which represents the combustion heat release as a large number of point sources convected by the resolvable flow field, is in fact a simple combustion model in its own right. It is consistent with more detailed combustion theories currently in use, and it permits the use of experimental data from fire experiments in a way that does not violate the consequences of those theories. A more detailed discussion of this model can be found in Ref. [5].

For a sprinkler spray, the force term \mathcal{F} in Eq. (2) is derived as follows: The momentum transferred from the water droplets to the gas is given by summing the force from each droplet in a control volume

$$\mathcal{F} = \frac{1}{2} \frac{\sum \rho c_d A_d \mathbf{u}_d |\mathbf{u}_d|}{V_{cv}} \quad (5)$$

where c_d is a drag coefficient, A_d is an effective cross sectional area of the particle, \mathbf{u}_d is the velocity of the droplet, and V_{cv} is the volume of the control volume. The trajectory of an individual droplet is governed by the equation

$$\frac{d}{dt}(m_d \mathbf{u}_d) = m_d \mathbf{g} - \frac{1}{2} \rho c_d A_d \mathbf{u}_d |\mathbf{u}_d| \quad (6)$$

where m_d is the mass of the droplet. The sprinkler spray droplet temperature T_d and radius r_d are governed by the following equations

$$\frac{dT_d}{dt} = \begin{cases} \frac{3 h_d}{c_w r_d \rho_d} (T_g - T_d) & T_d < T_v \\ 0 & T_d = T_v \end{cases} \quad (7)$$

$$\frac{dr_d}{dt} = \begin{cases} 0 & T_d < T_v \\ -\frac{h_d}{h_v \rho_d} (T_g - T_d) & T_d = T_v \end{cases} \quad (8)$$

where c_w is the specific heat of water, ρ_d is the density of the droplet, T_g is the gas temperature, T_v is the vaporization temperature of water, h_d is the heat transfer coefficient, given by

$$h_d = \frac{3 \text{Nu } k_a}{r_d}$$

Nu is the Nusselt number given by

$$\text{Nu} = 2 + 0.6 \text{Re}^{\frac{1}{2}} \text{Pr}^{\frac{1}{3}}$$

The Reynolds number is based on the velocity of the droplet with characteristic length $r_d/3$. The Prandtl number is about 0.7, and k_a is the thermal conductivity of air. The change in gas temperature due to the presence of the water droplets is given by

$$\frac{dT_g}{dt} = \sum \left(\frac{m_w}{m_a} \right) \left(\frac{c_w}{c_p} \right) \frac{3 h_d}{c_w r_d \rho_d} (T_d - T_g) \quad (9)$$

where m_w and m_a denote the mass of water and air in the control volume over which the summation is being performed. Of course, tracking every droplet is prohibitively expensive, and unnecessary. Instead, a sampling of the droplet population is tracked, with the characteristic parameters based on experimental measurements. This idea has been referred to as the “superdrop” concept [6]. It is directly analogous to the thermal element concept, and indeed tracking water droplets does not introduce any new machinery into the numerical code. In the calculations that will be discussed below, typically five to ten thousand droplets from each active sprinkler are tracked at any given time. This number of drops ensures that a sufficient distribution of the water is obtained.

Accurate prediction of sprinkler activation depends on both the accurate calculation of the gas temperature and velocity in the vicinity of the sprinkler, and on the characterization of the thermal properties of the sprinkler itself. The temperature of the thermal sensing element of the sprinkler is computed by solving the differential equation [7]

$$\frac{dT_l}{dt} = \frac{\sqrt{|u|}}{\text{RTI}} (T_g - T_l) - \frac{C}{\text{RTI}} (T_l - T_m) \quad (10)$$

Here T_l is the link temperature, T_g is the gas temperature in the neighborhood of the link, and T_m is the temperature of the sprinkler mount. The sensitivity of the detector is indicated by the value of RTI. The amount of heat conducted away from the link by the mount is indicated by the “C-Factor”, C . Both the RTI value and the C-Factor are determined from standardized plunge tests [8].

Liquid Fuel Burner Tests, January 1997

Heptane spray fire experiments were conducted at the large-scale fire test facility at Underwriters Laboratories, Chicago. The objective of the experiments was to characterize the temperature and flow fields for fire scenarios with a controlled heat release rate in the presence of vents and sprinklers. The results of the experiments are being used to check the predictive capability of the numerical model, and also provide guidance as to the interaction of vents and sprinklers when planning the full-scale commodity fires.

Twenty-two tests were conducted over an 8 day time period. The tests were conducted under the movable ceiling in the large test facility with a 4 ft by 8 ft vent among 49 sprinklers separated by 10 ft (see Fig. 1). The ceiling was instrumented with thermocouples at each sprinkler location, thermocouple trees at each fire location, velocity probes between the fire locations and the vent, and thermocouples and pressure taps above and below the vent.

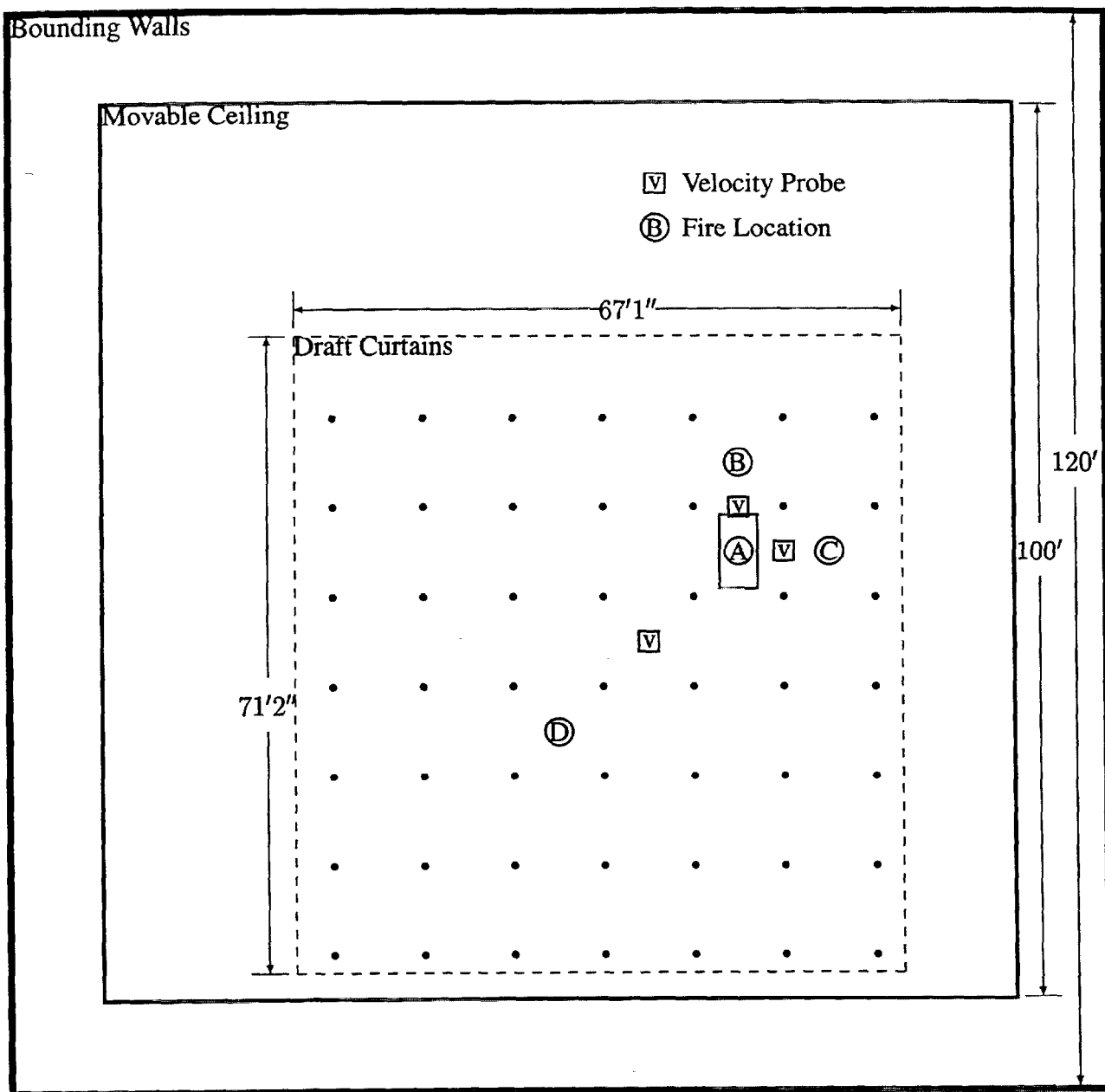


FIGURE 1: Plan view of UL heptane spray burner test configuration. The sprinklers are indicated by the solid circles and are spaced 10 ft apart. The vent dimensions are 4 ft by 8 ft. The numbered circles indicate burner positions.

In each test, the fire was positioned in one of four locations. The vent was either held closed, opened manually at a predetermined time, or allowed to open automatically. The manual vent opening times were chosen so that the vent would in one case be opened about 25 seconds prior to the first sprinkler activation (40 s), and in the other case about 25 seconds after the first sprinkler

activation (90 s). The fire growth curve used in all but one of the tests was of the form

$$\dot{Q} = \dot{Q}_0 \left(\frac{t}{\tau} \right)^2$$

where $\dot{Q}_0 = 10$ MW and $\tau = 75$ s. Following the activation of the first sprinkler, the heat release rate was held constant.

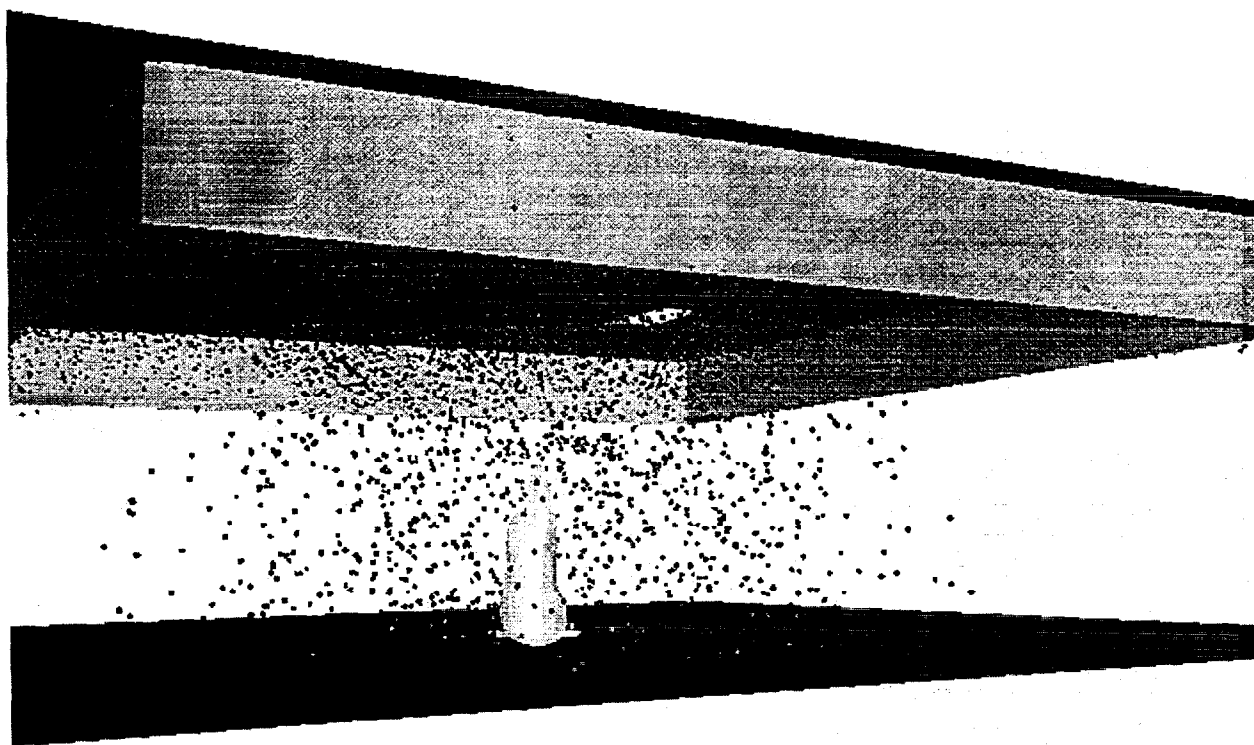
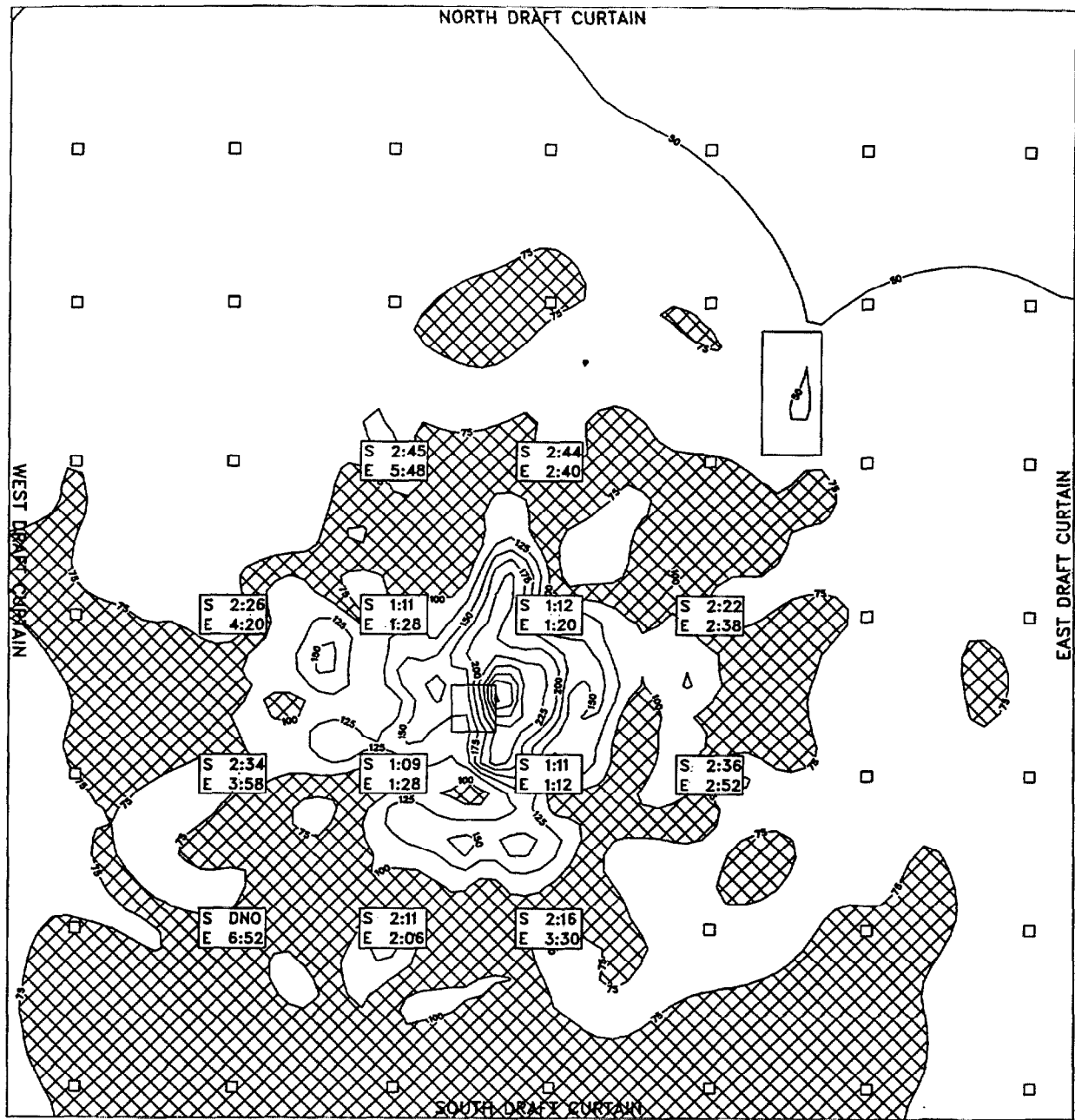


FIGURE 2: Numerical simulation of one of the UL heptane spray burner tests.

Numerical simulations of the experiments were performed before the tests began. However, due to difficulties controlling the flow of heptane to the burner, the heat release rates called for in the original test matrix could not be achieved. The calculations were re-run based on the actual recorded heptane flow rates. Tests are now underway to either confirm or refine estimates made of the convective heat release rate; and the RTI value, C-factor, drop size distribution, and density pattern of the extra-large orifice (ELO) sprinkler. The results of the calculations are very encouraging, and as more information becomes available on the sprinkler's thermal properties, the calculations will be redone to see how sensitive the results are to the changes.

The two figures on the following pages present the results of two of the tests. Figure 3 shows the sprinkler activation times from the simulation ("S") and the experiment ("E") at the locations of the activated sprinklers. The temperature contours are instantaneous snapshots from the simulation, showing the predicted temperatures near the ceiling at some arbitrary time during the simulation. Highlighted with a cross-hatched filling is the contour interval from 75°C to 100°C. The activation

TEST 10 (VENT OPENS AT 0:40, FAST FIRE AT LOCATION D, DRAFT CURTAINS)



NEAR-CEILING TEMPERATURE (C) AFTER 10 MINUTES

FIGURE 3: Comparison of sprinkler activation for a simulation (S) and one of the UL experiments (E). The contours represent an instantaneous snapshot of the near ceiling temperature. The cross-hatched area represents the interval between 75°C and 100°C. The fire was ramped up following a t-squared curve to a maximum of 4.45 MW in about 50 s. The vent was opened manually 40 s following ignition.

TEST 11 (NO SPRINKLERS, VENT OPENS AT 2:48, FAST FIRE AT D, DRAFT CURTAINS)

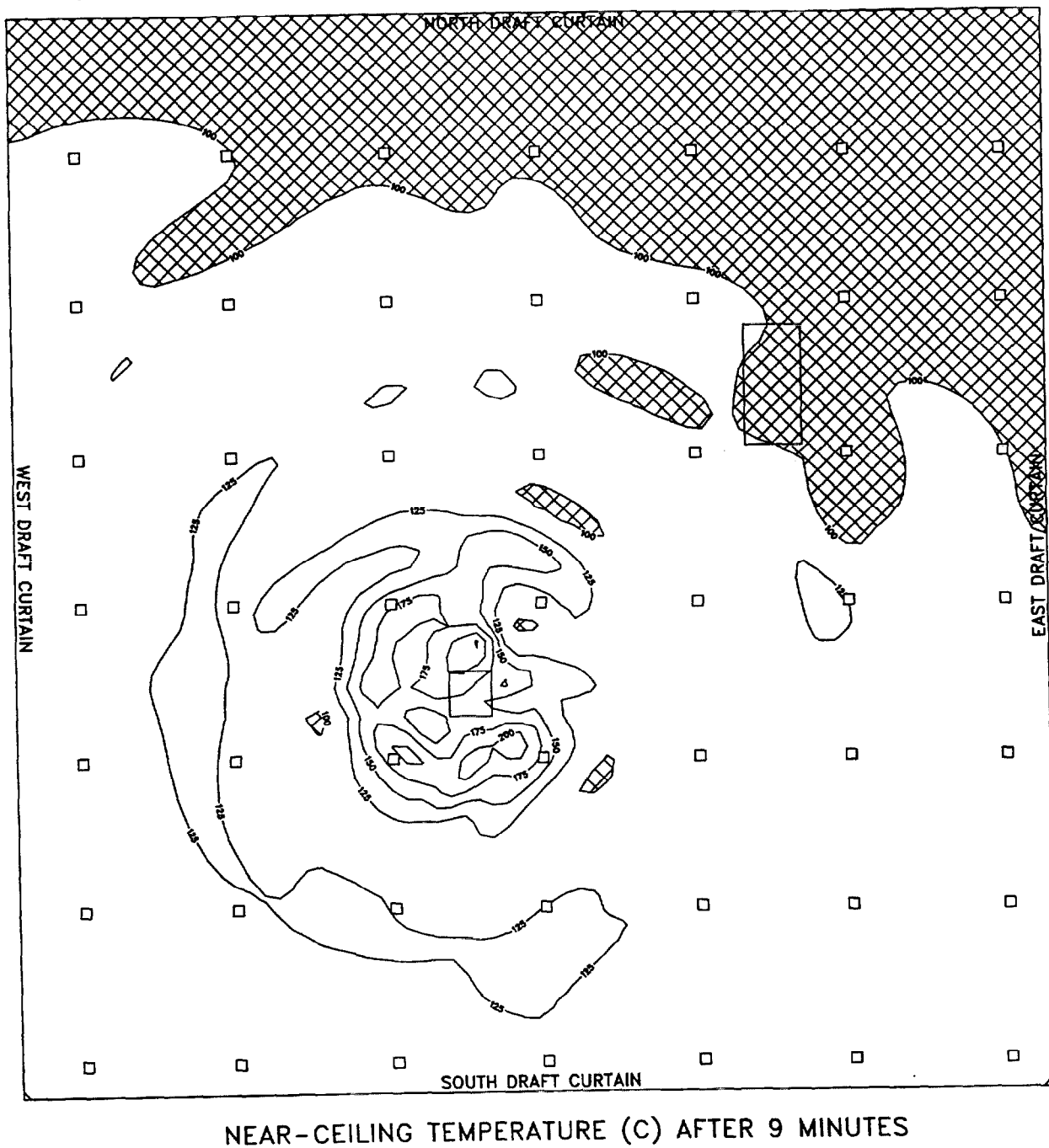


FIGURE 4: Near-ceiling temperatures from the simulation of a test in which no sprinklers were used. The contours represent an instantaneous snapshot of the near ceiling temperature. The cross-hatched area represents the interval between 75°C and 100°C. The fire was ramped up following a t-squared curve to a maximum of 4.45 MW in about 50 s. The vent was equipped with a 165°F link, and opened 2 minutes and 48 seconds following ignition.

time for the ELO upright sprinklers used in the tests is 74°C. The highlighted contour interval separates the area of almost certain activation from the area of almost no activation. It was observed during the tests that following the activation of the 4 sprinklers nearest the fire after about 65 seconds, the sprinklers in the next ring would activate if the surrounding gas temperature was at least 90°C. Thus, the 75–100°C interval represents an area of possible activation. Figure 4 presents the near-ceiling temperatures from a simulation of a test performed with no sprinklers in place. Comparing Figure 3 and Figure 4 indicates the overall cooling effect of the activated sprinklers.

The results summarized in Figure 3 reveal the promise and the limitations of predicting sprinkler response. Most notably, the experimental activation times do not necessarily reflect the symmetry of the layout. Because the burner was positioned directly in the center of four sprinklers, there is no reason to expect the kind of time differences between neighboring sprinklers, unless the fire plume was biased in one particular direction. It was noticed during the tests that the plume would indeed lean, due probably to asymmetric air intake flow rates. The weather in Chicago during the week of testing was bitterly cold and windy, causing some draft in the test facility. The model cannot predict this type of bias unless that information is available. In the absence of such information, the activation times will, in this case, follow a relatively symmetric pattern. Consider, for example, the gas temperatures in the vicinity of two neighboring sprinklers, shown in Figure 5. Referring to Figure 3, the two sprinklers are the third and fourth in the second row from the bottom. The simulation does not show any difference in temperature at the two locations. However, the temperature increases about 10° for about 20 seconds over the corresponding location. Apparently, this is the reason for the earlier activation.

Conclusions

The data from the UL heptane tests is still being evaluated. Plunge tests are now being conducted on the specific sprinkler used in the tests to determine its thermal properties (estimates were used in the simulations performed to date). The comparisons between model and experiment are encouraging, and they provide some guidance into how well any model can be expected to predict multiple sprinkler activation. As was seen in the sample calculation presented above, the model cannot predict exactly the activation times of the sprinklers because of the inherent fluctuations in the test conditions and the thermal response of the sprinklers. However, it is hoped that the model prediction falls within the uncertainty intervals of the experimental data.

References

- [1] H.R. Baum, O.A. Ezekoye, K.B. McGrattan, and R.G. Rehm. Mathematical modeling and computer simulation of fire phenomenon. *Theoretical and Computational Fluid Dynamics*, 6:125–139, 1994.
- [2] K.B. McGrattan, R.G. Rehm, and H.R. Baum. Fire-driven flows in enclosures. *Journal of Computational Physics*, 110(2):285–292, 1994.
- [3] K.B. McGrattan, R.G. Rehm, and H.R. Baum. Mathematical modeling and computer simulation of fire phenomenon. In Takashi Kashiwagi, editor, *Proceedings of the 4th International*

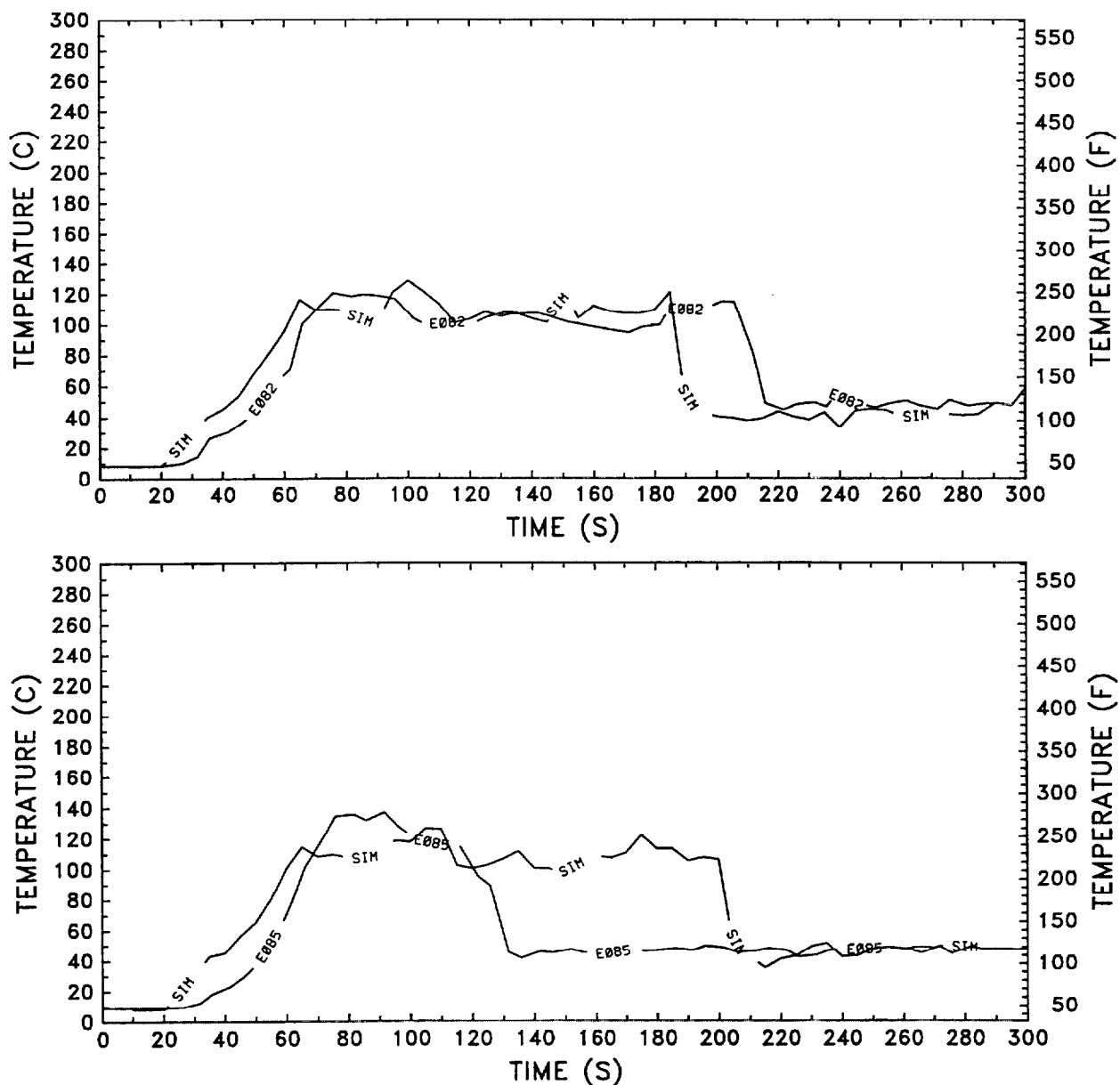


FIGURE 5: Comparison of gas temperatures of experiment (E) and simulation (SIM). The first plot shows temperatures near the third sprinkler in the second row from the bottom of Figure 3. The second plot shows temperatures near the fourth sprinkler in the second row from the bottom.

Symposium on Fire Safety Science, pages 185–194. International Association of Fire Safety Science, 1994.

[4] R.G. Rehm and H.R. Baum. The equations of motion for thermally driven, buoyant flows. *Journal of Research of the NBS*, 83:297–308, 1978.

[5] H.R. Baum, K.B. McGrattan, and R.G. Rehm. Large eddy simulations of smoke movement in three dimensions. In *Proceedings of the Seventh International Interflam Conference*, pages

189–198. Interscience Communications, London, 1996.

- [6] S. Kumar, G.M. Heywood, S.K. Liew, and W.S. Atkins. Jasmine sprinkler model - some validation studies. In *Proceedings of the First European Symposium on Fire Safety Science*, 1995. ETH, Zurich.
- [7] G. Heskestad and R.G. Bill. Conduction heat loss effects on thermal response of automatic sprinklers. Technical report, Factory Mutual Research Corporation, September 1987.
- [8] International Organization for Standardization (ISO), Geneva, Switzerland. *Fire Protection – Automatic Sprinkler Systems – Part 1: Requirements and test methods for sprinklers, ISO 6182-1*, 1993.